On the Work-Hardening Mechanism of TWIP Steels Strengthened by Nanometre-Sized Vanadium Carbides

Z.Y. Liang[1], M.X. Huang[1*], H.W. Yen[2], C. P. Scott[2]

(1. Department of Mechanical Engineering, The University of Hong Kong, Hong Kong, China;
2. Australian Centre for Microscopy & Microanalysis, The University of Sydney, NSW, 2006, Australia;
3. Areva NP, 10 rue Juliette Récamier, 69456 LYON, France)

Abstract: Experiments reveal that while dispersed nanometer-sized vanadium carbides can greatly increase the yield strength of twinning induced plasticity (TWIP) steels, they may cause some reduction of the overall work-hardening rate. A modified physically based model is adopted in the present work to capture the effect of nanometer-sized vanadium carbides on the work-hardening rate of a laboratory FeMnC austenitic TWIP grade. It is found that the introduction of the dispersed nanometer-sized carbides leads to a faster dislocation accumulation rate but reduces the rate of twin formation with strain during plastic deformation. Compared to a reference alloy without precipitates the work-hardening rate is higher at small strains but decreases faster than the reference thus presenting a lower work-hardening rate at high strains.
Key words: TWIP steels, Vanadium carbides, Work-hardening, Dislocation evolution, Twinning kinetics

1 Introduction

Twinning induced plasticity (TWIP) steel are promising structural materials for automotive applications due to their excellent combination of strength and ductility [1] (a true stress of 1726 MPa with true strain of 0.491 at fracture has been obtained in this research). The implementation of TWIP steels in automotive applications could be retarded by their relatively low yield strengths (YS), especially for anti-intrusion components in the body-in-white [1, 2]. Feasible ways to improve the YS of the TWIP steels such as pre-straining by cold work and grain refinement turn out to have certain limits. For example, pre-straining strongly reduce the formability by increasing the plastic anisotropy[2], and the amount of grain refinement attainable by current industrial cold strip processing lines is insufficient to achieve the required YS for many automotive applications (600~700 MPa)[1]. Precipitate strengthening is another possible way to improve the YS in TWIP steels[1-3]. In our previous research [3], the YS increment obtained by introducing a dispersion of nanometer-sized vanadium carbides was estimated to be about +200 MPa. The research of Bouaziz et al. further showed that vanadium additions, when coupled with suitable additions, can increase the YS by up to 375 MPa before saturation effects become dominant [1]. In these tests the uniform elongation was still > 40%. However, experimental observations also reveal that the introduction of carbides to the austenite matrix may lead to a decrease of the work-hardening rate[2]. In the research of Scott et al., the reduction of the work-hardening rate at large strains (ε >0.3) may be due to the complex interaction between carbides and mechanical twins or stacking faults. Since mechanical twinning has a pronounced effect on the work-hardening rate of TWIP steels as described by the dynamic Hall-Patch effect [4], one possible explanation for the decrease of the work-hardening rate at high strains in TWIP steels with nanometer-sized carbides is that these precipitates may reduce the rate of twin formation during deformation. Scott et al.[2] showed using synchrotron X-ray diffraction that, at the same tensile strain, the density of mechanical twins/stacking faults in a TWIP steel with nanometer-sized carbides was lower than that of a reference

* Corresponding author: mxhuang@hku.hk

alloy without carbides. In addition, dispersed carbides can effectively reduce the mean free path (MFP) for dislocation glide so that the evolution of the dislocation density during plastic deformation might also be affected by the addition of nanometer-sized carbides. This is another important mechanism contributing to the work-hardening rate. A proper physically based model incorporating the effect of nanometer-sized carbides on the twinning kinetics and dislocation evolution can describe the change of the work-hardening rate. The aim of the present study is to capture the effect of precipitates on the work-hardening rate of TWIP steels by a modified model incorporating the effect of nanometer-sized vanadium carbides on the twinning kinetics and dislocation evolution. Two TWIP steels (with and without nanometer-sized carbides) were chosen for the modeling analysis.

2 Modeling

The flow stress during plastic deformation is a combination of three stress components [5]:

$$\sigma = \sigma_0 + \sigma_f + \sigma_b \tag{1}$$

σ_0 is, in general, a given constant representing the lattice friction stress due to the solid solution. Nevertheless, for TWIP steel with dispersed carbides, σ_0 should also include an extra resistant stress that dislocations need to overcome when they by-pass the carbides according to the Orowan mechanism [6]. σ_f is related to the isotropic hardening due to the interaction of a moving dislocation with the forest dislocations. σ_b is the back stress induced by dislocation pile-ups against grain or twin boundaries. The isotropic hardening stress component is proportional to the square root of the statistical stored dislocation density ρ so that [5]:

$$\sigma_f = M\alpha Gb\sqrt{\rho} \tag{2}$$

α is a factor related to the dislocation structure, M is the average Taylor factor, G is the shear modulus and b is the Burgers vector of a perfect dislocation. Both the grain and twin boundaries are effective barriers for dislocation motion. It is assumed in this model that dislocations will be stopped at these boundaries and the back stress caused by the dislocation pile-ups against the boundaries can be expressed as [7]:

$$\sigma_b = M\frac{Gb}{L}n \tag{3}$$

Here n represents the number of dislocations that pile up against a boundary. For simplification, the evolution of n is neglected and n is assumed to be equal to n_o (the maximum number of pile-up dislocations, used as fitting parameter in this model) right from the onset of plastic deformation. L is the geometric length scale of the microstructure. For this model, the twin and grain boundaries are assumed to be the dominant barriers for dislocation glide. Therefore L can be constructed as [4, 7]:

$$\frac{1}{L} = \frac{1}{d} + \frac{1}{t} \tag{4}$$

where d is the grain size and t is the average twin spacing. Based on the stereological analysis of Fullman, the average twin spacing has a relationship with the twin volume fraction F and twin thickness e (assumed constant) as follow [8]:

$$\frac{1}{t} = \frac{1}{2e}\frac{F}{(1-F)} \tag{5}$$

The average shear strain during plastic deformation includes contributions from both dislocation glide and deformation twinning and is linked to the macroscopic strain by the average Taylor factor [5]:

$$d\varepsilon = M\cdot((1-F)d\gamma_g + dF\cdot d\gamma_t) \tag{6}$$

where γ_g is the shear strain by dislocation glide, γ_t is the twinning shear strain equal to $1/\sqrt{2}$ and F is the twin volume fraction. The dislocation evolution is the competition between the multiplication and dynamic recovery of the statistical stored dislocations [7]:

$$d\rho = d\gamma_g\cdot(\frac{k}{b}\sqrt{\rho} - f\rho) \tag{7}$$

where k and f are factors related to the athermal work-hardening limit and dynamic recovery respectively. In this model, f is set the same for both steels while k is set as a fitting parameter to evaluate the effect of the carbides on the dislocation evolution. The twinning kinetics model is based on the twinning mechanism proposed by Majahan and Chin [9]. A three-layer twin nucleus may form when two perfect

dislocations split into fault pairs and react on the primary slip plane. Before this twin nucleus can further grow into a microscopic twin, the twinning partials of the nucleus need to bow out from their pinning points and the critical shear stress for this event is (detailed derivation of this critical stress can be found in [10]):

$$\tau_C = \frac{\gamma_{sf}}{\partial b_s} + \frac{\hat{\partial} G b_s}{L_0} \tag{8}$$

where γ_{sf} is the stacking fault energy, b_s is the Burgers vector of the twinning partials and L_0 is the distance between the two pinning points of the twinning partials. Considering the nature of L_0, it is reasonable to assume that this distance is related to the MFP for dislocation motion and can be constructed in a similar way to include a contribution from the distance between the carbides, the dislocation density, the twin spacing and the grain size:

$$\frac{1}{L_0} = \frac{1}{\lambda} + \frac{\sqrt{\rho}}{i_C} + \frac{1}{t} + \frac{1}{d} \tag{9}$$

where λ is the average surface to surface distance between carbides and i_C is a factor (fitting parameter) for scaling the influence of the mean dislocation space in L_0. For the TWIP steel without carbides, λ is set as a fitting parameter. According to Steinmetz et al.[10], the number density of potential twin nucleii that form during a small strain is equal to the number of events occurring where two repulsive perfect dislocations with the length of L_0 meet and react with each other within a unit volume:

$$\theta = \frac{56}{110}\frac{d\gamma_g}{2}\frac{2}{3L_0}\rho \tag{10}$$

The effective twin nucleii should be the ones that are able to overcome the energy barriers when they bow out. The probability of this event can be expressed by an exponential function as:

$$p_{tw} = \exp[-(\frac{\tau_c}{\tau_{rss}})^s] \tag{11}$$

s is a factor for determining the sharpness of the transition from the non-twinning to the twinning domain. τ_{rss} is the average resolved shear stress and can be related to the external flow stress by the average Taylor factor:

$$\tau_{rss} M = \sigma \tag{12}$$

Therefore the number density of effective twin nuclei should take into account of the number density of potential twin nucleii and the probability that the resolved shear stress can provide enough driving force for a twin nucleus to grow:

$$N = \theta p_{tw} \tag{13}$$

The twin is assumed to have a disc-shape the dimensions of which are dependent on the average twin spacing. The twin volume is given as follows:

$$V_{tw} = \frac{\pi}{4} e t^2 \tag{14}$$

Finally, we assume that new twins can only form in the untwined non-twined volumes and the twin volume fraction can be calculated by:

$$dF = (1 - F) N V_{tw} \tag{15}$$

3 Results and Discussion

The two TWIP steels chosen for current work are Fe-21.6Mn-0.65C (wt.%) (referred to as TWIP1 hereafter) and Fe-21.8Mn-0.63C-0.87V (wt.%) (referred to as TWIP2 hereafter) with a grain size of 2.5 μ m and 1.2 μ m respectively. For TWIP2, the average size of the vanadium carbides is 13 ± 7.7nm and the carbide number density is 4.7×10^3 μ m^{-3} determined by transmission electron microscopy (TEM) characterization [3]. The average surface to surface distance between carbides is estimated to be 117nm. The true stress-strain data of both TWIP steels are utilized to optimize the fitting parameters in the model. The physically based constants and fitting parameters used in the model are listed in Table 1.

The modeling and experimental results on true stress-strain curves and work-hardening rates are shown in Fig. 1. The modeling results show a good fit with both the true stress-strain curves and the work-hardening rates of both steels. For both alloys, the work-hardening rate decreases continuously with strain until it intersects with the true stress-strain curve at which fracture happens. Comparing the two steels, TWIP2 has a higher work-hardening rate than TWIP1 at small strains. However, as straining progresses, it decreases at a much higher rate and becomes lower than that of TWIP1 after a strain of

about 10%. Considering equation (1), only σ_f and σ_b can make contribution to the work-hardening rate (σ_0 is a constant). By differentiating σ_f with strain (ε) and combining with equation (7), the change of the forest hardening stress with strain ($d\sigma_f/d\varepsilon$) can be obtained as follows:

$$\frac{d\sigma_f}{d\varepsilon} = \frac{M^2\alpha Gb}{2}\left(\frac{k}{b} - f\sqrt{\rho}\right) \tag{16}$$

Table I Value of the physical constants and the fitting parameters in the model*

Parameters	Description	Value
G	Shear modulus/GPa	65
b	Burgers vector/m	2.54×10^{-10}
M	Average Taylor factor	3.08
α	Mean dislocation strength	0.4
d	Grain size/ μ m	2.5/1.2
f	Dynamic recovery factor	3
e	Twin thickness/ nm	30
γ_{sf}	Stacking fault energy/mJ·m^{-2}	22
λ	Average surface to surface distance of carbides/nm	243/117
n_o	Maximum number of pile-up dislocations	1.6/ 1.3
k	Forest hardening factor	0.025/ 0.039
i_c	Scaling factor of dislocation space for L_0	4.91
s	Transition profile width exponent	20.85

* Values in the first part are the adopted physics-based constants and values in the second part are the fitting parameters except that the average surface to surface distance between carbides for TWIP2 is determined by TEM. If there are two values in the same row, this first and second one is for TWIP1 and TWIP2 respectively.

The simulation result shows that TWIP2 has a larger k than TWIP1 (see Table 1). Since k is a factor for scaling the influence of the mean dislocation spacing on the MFP of dislocation motion, the steel containing carbides that can certainly further reduce the MFP will naturally have a larger k value. In addition, TEM characterization [3] reveals that the dispersed nanometer-sized carbides in TWIP2 are non-shearable which means that large amount of geometrically necessary dislocations (GND) may be induced during plastic deformation according to the Oroman mechanism [6]. With a larger k, $d\sigma_f/d\varepsilon$ for TWIP2, based on equation (16), will have a larger initial value (both the dynamic recovery factor and the initial dislocation density are set equal for both steels). However, as the strain increases, TWIP2, faster accumulation of the dislocations (Fig. 2.) due to a larger k will in return show a faster reduction of $d\sigma_f/d\varepsilon$.

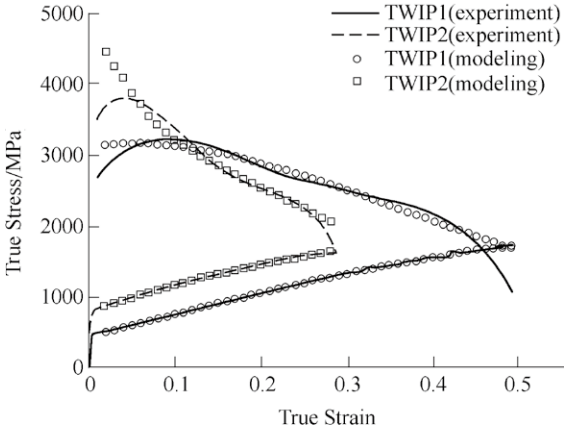

Fig. 1 Comparison of the experimental and modeled tensile and work-hardening behavior for both steels

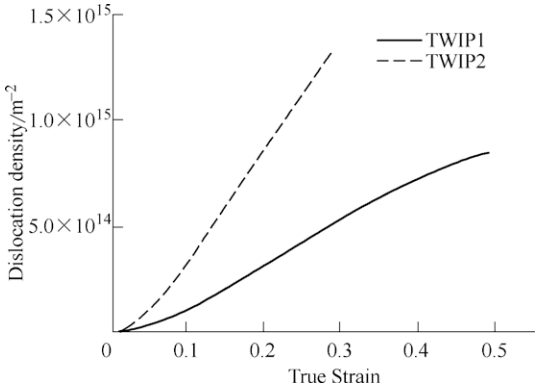

Fig. 2 Calculated dislocation density evolution for both steels

Based on equation (3) the change of the back stress (σ_b) with strain (ε) is controlled by the evolution of L with strain (n is equal to n_o and does not change with strain) and L is mainly affected by the twin volume fraction F. By differentiating σ_b with ε and combining with equation (4) and (5), the change of σ_b with ε can be obtained:

$$\frac{d\sigma_b}{d\varepsilon} = \frac{MGbn_0}{2e}\left(\frac{1}{(1-F)^2}\cdot\frac{dF}{d\varepsilon}\right) \tag{17}$$

For the comparison of $d\sigma_b/d\varepsilon$ for both steels, the problem can be further simplified by assuming a linear increase of the twin volume fraction with strain, this causes $dF/d\varepsilon$ to be a constant, v. As shown in Fig. 3, TWIP2 has much lower twin volume fraction than that of TWIP1, which is attributed to dispersed nanometer-sized carbides in the current model. Careful TEM

characterization in our previous work [3] has revealed the strong interaction between the twinning partials and vanadium carbides. The extra stress needed for a twinning partial to by-pass the carbides is large (598MPa) and will probably suppress the twin growth at both the edge and facial direction, resulting in a lower twin volume fraction. Evaluated with Fig. 3., the twinning constant for TWIP1 (v_1=0.69) is nearly two times that for TWIP2 (v_2=0.36). By substituting the required values into equation (17), it is clear that TWIP1 has a larger $d\sigma_b/d\varepsilon$ than TWIP2.

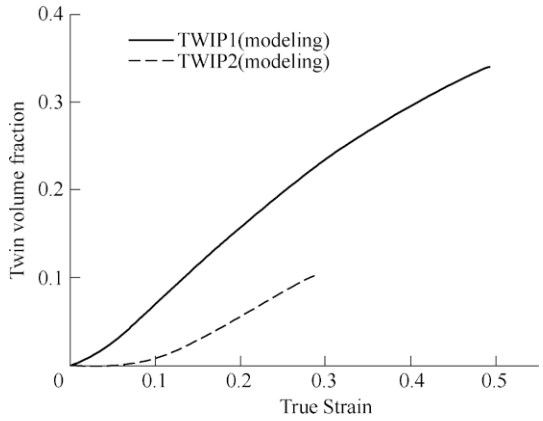

Fig.3 Calculated evolution of the twin volume fraction with strain for both steels

Fig. 4. summarizes the evolution of $d\sigma_f/d\varepsilon$ and $d\sigma_b/d\varepsilon$ for both steels. The overall work-hardening rate shown in Fig. 1 is equal to the addition of $d\sigma_f/d\varepsilon$ and $d\sigma_b/d\varepsilon$ with a small gap resulting from the simplification of $dF/d\varepsilon$. Although the work-hardening rate for TWIP2 has a larger initial value due to a larger *k*, it decreases much faster with strain due to faster dislocation evolution and lower twinning kinetics.

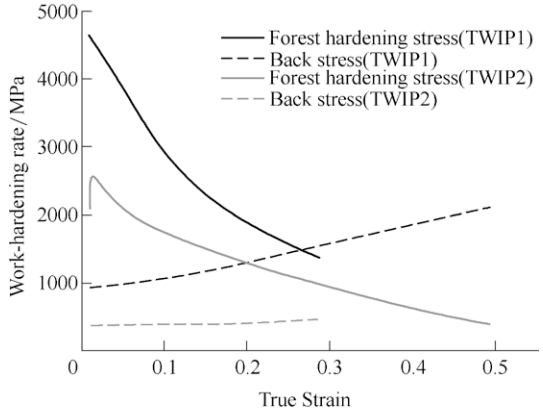

Fig. 4 Calculated contributions to the work-hardening rate from σ_f and σ_b for both steels

4 Conclusion

The present work applies a modified physically based model to capture the effect of nanometer scale vanadium carbides on the work-hardening behavior of FeMnC austenitic TWIP steels. The model shows a good fit with the experimental measurements of true stress-strain curves and work-hardening rates. It is found that the introduction of the dispersed nanometer-sized carbides results in a faster dislocation evolution process but reduces the rate of twin nucleation during plastic deformation. The consequence is a larger work-hardening rate at the start of plastic deformation and a quicker decrease as strain proceeds leading to a smaller work-hardening rate at large strains. This model is useful to determine the optimum precipitate distribution (mean size, number density) for a target set of mechanical (tensile) properties. When coupled with suitable kinetic thermodynamic precipitation models, it should facilitate the definition of the nominal microalloying content and required thermal processing parameters in an integrated alloy design approach.

References

[1] Bouaziz O, Allain S, Scott CP, Cugy P, Barbier D. Current Opinion in Solid State and Materials Science 2011;15:141.

[2] Scott CP, Remy B, Collet JL, Cael A, Bao C, Danoix F, Malard B, Curfs C. Precipitation strengthening in high manganese austenitic TWIP steels. Int.J.Mat.Res. 102 5 pp538~549.

[3] Yen H-W, Huang M, Scott CP, Yang J-R. Scripta Materialia 2012;66:1018.

[4] Bouaziz O, Guelton N. Materials Science and Engineering: A 2001;319~321:246.

[5] Bouaziz O, Allain S, Scott C. Scripta Materialia 2008;58:484.

[6] Orowan E in: Martin JW (Ed.). Precipitation Hardening. Oxford: Pergamon Press, 1968.

[7] Estrin Y, Meching H. Acta Materialia 1984;32:57.

[8] Fullman RL. Trans. AIME 1953;197:447.

[9] Mahajan S, Chin GY. Acta Metallurgica 1973;21:1353.

[10] Steinmetz DR, Jäpel T, Wietbrock B, Eisenlohr P, Gutierrez-Urrutia I, Saeed–Akbari A, Hickel T, Roters F, Raabe D. Acta Materialia 2013;61:494.